

Fano resonances as a probe of phase coherence in quantum dots

A. A. Clerk, X. Waintal, P. W. Brouwer

Laboratory of Atomic and Solid State Physics, Cornell University, Ithaca NY 14853, USA

(Jan 5, 2001)

In the presence of direct trajectories connecting source and drain contacts, the conductance of a quantum dot may exhibit resonances of the Fano type. Since Fano resonances result from the interference of two transmission pathways, their lineshape (as described by the Fano parameter q) is sensitive to dephasing in the quantum dot. We show that under certain circumstances the dephasing time can be extracted from a measurement of q for a single resonance. We also show that q fluctuates from level to level, and calculate its probability distribution for a chaotic quantum dot. Our results are relevant to recent experiments by Göres *et al.*

PACS numbers: 73.20.Dx., 73.23.Hk, 73.40.Gk

Perhaps one of the most fundamental issues in the field of mesoscopic physics is that of phase coherence: under what conditions are electrons able to retain a well-defined phase? This issue is of particular interest for quantum dots in the Coulomb blockade regime, where the electrical conductance is suppressed except for points of charge degeneracy [1]. Despite the fact that interactions are strong in these dots, the shape of the conductance peaks can be well understood in terms of single-particle wavefunctions. Unfortunately, a simple conductance measurement cannot discriminate between coherent and incoherent (sequential) tunneling, as both mechanisms give rise to lineshapes of Breit-Wigner form [2]. Instead, to establish phase coherence, the quantum dot has to be embedded in an interferometer. This was first done by Yacoby *et al.* [3], who included a quantum dot in one arm of an Aharonov-Bohm ring (see also Ref. [4]).

Given this result, it is natural to question the *extent* to which transport is phase coherent. This question could not be fully addressed in Ref. [3], because dephasing in the quantum dot and in the arms of the interferometer cannot easily be separated. An extremely promising development in this respect is found in a recent work by Göres *et al.* [5], who observed resonances with a Fano lineshape in the conductance of Coulomb-blockaded dots [6], instead of the usual Breit-Wigner form. Fano resonances are caused by the interference of two transport pathways, a resonant and a nonresonant one, and are thus sensitive to phase coherence. In the dots of Ref. [5], the direct pathway is probably direct transmission through the dot, as schematically depicted in Fig. 1. In this sense, the dot serves as its own interferometer!

Fano resonances have a lineshape of the form

$$G(\varepsilon) = G_d \frac{|2\varepsilon + q\Gamma|^2}{4\varepsilon^2 + \Gamma^2}, \quad (1)$$

where G is the conductance, measured in units of $2e^2/h$, ε the energy, set by a gate voltage, Γ the resonance width, G_d the nonresonant conductance, and q the (complex) ‘‘Fano parameter’’. The resonance form (1) arises from the interference of a ‘‘direct’’ nonresonant path with

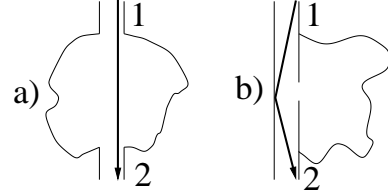


FIG. 1. Schematic drawing of two quantum dot systems in which Fano resonances are expected. a) A dot similar to that used in a recent experiment by Göres *et al.* [5], showing a possible direct path (d). b) A system where the width of Fano resonances can be tuned without altering the direct path.

transmission amplitude $t_d = e^{i\beta_a} \sqrt{G_d}$ and a resonant path with transmission amplitude $t_r(\varepsilon) = z_r \Gamma / (2\varepsilon + i\Gamma)$, where $G(\varepsilon) = |t_d + t_r|^2$ and $q = i + z_r e^{-i\beta_a} / \sqrt{G_d}$. The Fano lineshape (1) is for temperatures $T \ll \Gamma$, which is appropriate for the experiments on very small quantum dots of Refs. [3–5]. Examples of dots that could show Fano resonances are shown in Fig. 1. The example of Fig. 1b is particularly interesting, as it allows one to control the width of the Fano resonances by varying the size of the contact to the cavity.

Through the complex Fano parameter q , Fano resonances contain more information than Breit-Wigner resonances. Moreover, as the direct and resonant paths are not spatially separated, no source of decoherence other than dephasing inside the quantum dot can affect the lineshape. In fact, as we will show below, in the presence of time-reversal symmetry (TRS) or for a dot of the form of Fig. 1b, where the opening to the cavity contains at most one propagating channel, measurement of a single Fano resonance at $T \ll \Gamma$ is sufficient to determine the dephasing time τ_ϕ in the quantum dot:

$$\frac{\hbar}{\tau_\phi} = \Gamma \left(|q|^2 + 1 - \sqrt{(|q|^2 + 1)^2 - 4(\text{Im } q)^2} \right). \quad (2)$$

In this letter, we develop a detailed description of Fano resonances in quantum dots. In addition to the effect of dephasing, we consider mesoscopic fluctuations — the Fano parameter q and the width Γ fluctuate from reso-

nance to resonance. We calculate the probability distribution of q for a set of consecutive resonances in a chaotic quantum dot using random matrix theory. We close with a comparison of our results and the experiment of Ref. [5]. Several previous studies have treated Fano resonances in quasi-one-dimensional systems rather than quantum dots [7] and without mesoscopic fluctuations or dephasing.

Model. We consider a quantum dot coupled to two single-mode leads (1 and 2) via point contacts, see Fig. 1. Transport through the system is characterized by the 2×2 scattering matrix $S(\varepsilon)$, which we parameterize in terms of a (unitary) scattering matrix $S_0(\varepsilon)$ for processes that involve ergodic exploration of the cavity, and a (non-unitary) matrix \bar{S} that describes scattering via the direct, non-resonant paths (both transmitting and reflecting) [8,9],

$$S = \bar{S} + t' \frac{1}{1 - S_0 r'} S_0 t. \quad (3)$$

The auxiliary matrix t describes transmission from the leads to an ergodic dot state, while t' describes transmission from such a state back into the leads. Similarly, r' describes reflection of an electron leaving an ergodic dot state back into the dot. Our results are independent of t' , t , and r' , as long as the 4×4 matrix

$$\begin{pmatrix} \bar{S} & t' \\ t & r' \end{pmatrix}$$

is unitary. As the time scale of the direct processes is much smaller than \hbar/Δ , where Δ is the level spacing of the dot, \bar{S} will be constant over an energy interval spanning a large number of distinct resonances. Also, since TRS cannot be broken on this short time scale, \bar{S} is symmetric. In contrast, the scattering matrix S_0 , which describes scattering from long, resonant paths, depends on energy and is only symmetric in the absence of a TRS breaking magnetic field. We use the polar decomposition of \bar{S} [9],

$$\bar{S} = U \sqrt{(1 - T)} U^T, \quad (4)$$

where U is a 2×2 unitary matrix and $T = \text{diag}(T_1, T_2)$. Without loss of generality, we may choose $t' = t^T = U \sqrt{T}$, $r' = -\sqrt{1 - T}$. The numbers $0 \leq T_1 \leq T_2 \leq 1$ are known as “sticking probabilities” [10], i.e., the probabilities for scattering through paths that explore the dot ergodically, instead of direct transmission via a short path. (The inequality $T_1 \leq T_2$ is made for definiteness.) The standard theory of Fano resonances [6] (see also [7]) assumes the existence of a single sticking probability only. In our case, the existence of two sticking probabilities T_1 and T_2 follows because the dot is coupled to two single-mode leads. We assume $T_1, T_2 \ll 1$, which ensures that the resonances are narrow and well-separated.

For S_0 , we make use of the formula [9]

$$S_0(\varepsilon) = [1 - iK(\varepsilon)] / [1 + iK(\varepsilon)], \quad (5)$$

where K is a 2×2 matrix representing the Green function of the closed cavity at the contacts [11]. A resonance occurs when K has a pole, i.e., when ε coincides with an energy level of the closed dot. Close to resonance, $K \simeq \Delta \Psi \Psi^\dagger / (\pi \varepsilon)$, where the two-component vector $\Psi = (\Psi_1, \Psi_2)$ represents the values of the wavefunction at the leads. For convenience, we have set the resonance energy to zero. Then $S(\varepsilon)$ takes the form

$$S(\varepsilon) = U \left(1 - \frac{2i\Delta\sqrt{T}\Psi\Psi^\dagger\sqrt{T}}{4\pi\varepsilon + i2\pi\Gamma} \right) U^T, \quad (6)$$

where $\Gamma = \Delta \Psi^\dagger T \Psi / 2\pi$. By the Landauer formula, $S(\varepsilon)$ determines the conductance $G(\varepsilon) = |S(\varepsilon)_{12}|^2$, and hence the Fano parameter q . Far from resonance, the second term in Eq. (6) vanishes, so that the non-resonant contribution to the conductance reads $G_d = |(UU^T)_{12}|^2$.

Several conclusions can be drawn directly from Eq. (6). First, writing $q = q_x + iq_y$, unitarity of S implies that q_x and q_y are bounded. Defining $(q_x^{\text{max}})^2 = (q_y^{\text{max}})^2 - 1 = 1/G_d - 1$, and changing to “normalized” real and imaginary parts of the Fano parameter $\tilde{q}_x = q_x/q_x^{\text{max}}$, $\tilde{q}_y = q_y/q_y^{\text{max}}$, Eq. (6) gives the constraint

$$\tilde{q}_x^2 + \tilde{q}_y^2 \leq 1. \quad (7)$$

Second, in the presence of TRS, the wavefunction Ψ can be chosen real, from which one finds $q_y = 0$. This implies that, in the absence of dephasing, the conductance drops to zero at $\varepsilon = -q_x \Gamma / 2$.

Resonance-to-resonance fluctuations. We now consider a set of consecutive resonances in a single quantum dot, all occurring within an energy interval in which \bar{S} can be considered constant. In general, the Fano parameter q is sensitive to the resonance wavefunction Ψ only through the ratio $T_1 \Psi_1 / T_2 \Psi_2$. If one of the sticking probabilities is zero, so that the resonant state is only coupled to the outside world via a single channel, this ratio is independent of Ψ , and q is set solely by the direct process. This results in q being real and the same for each resonance:

$$q = q_a = i(U_{11}U_{21} - U_{22}U_{12}) / (U_{11}U_{21} + U_{22}U_{12}). \quad (8)$$

In quantum dots, this limit can be realized, for example, in the geometry of Fig. 1b, if the opening to the cavity supports only one mode at the Fermi level. However, in the generic case (if the opening contains more than one mode, or in the geometry of Fig. 1a), both sticking probabilities T_1 and T_2 are nonzero. Then q depends on the wavefunction of the resonance, and should exhibit mesoscopic fluctuations from resonance to resonance. In the case of a chaotic quantum dot, we obtain the distribution of q for our set of resonances by using random matrix theory (RMT) for the statistics of the wavefunction Ψ [12], keeping \bar{S} the same for all resonances (and hence U

and T). According to RMT, the elements of Ψ are independently distributed real (complex) Gaussian random numbers with zero mean and unit variance, in the presence (absence) of TRS. In terms of the normalized real and imaginary parts \tilde{q}_x and \tilde{q}_y , and with $\tilde{q}_a = q_a/q_x^{\max}$, we find that in the presence of TRS the distribution P is given by

$$P = \frac{1}{\pi} \sqrt{\frac{1+\alpha}{1-\tilde{q}_x^2}} \frac{1 + \frac{\alpha}{2}(1-\tilde{q}_x\tilde{q}_a)}{1 + \alpha(1-\tilde{q}_x\tilde{q}_a) + \frac{\alpha^2}{4}(\tilde{q}_x - \tilde{q}_a)^2} \delta(\tilde{q}_y), \quad (9a)$$

while in the absence of TRS

$$P = \frac{1+\alpha}{2\pi\sqrt{1-\tilde{q}_x^2-\tilde{q}_y^2}} \times \frac{[1 + \frac{\alpha}{2}(1-\tilde{q}_x\tilde{q}_a)]^2 + \frac{\alpha^2}{4}(1-\tilde{q}_x^2-\tilde{q}_y^2)(1-\tilde{q}_a^2)}{[1 + \frac{\alpha^2}{4}[(\tilde{q}_x - \tilde{q}_a)^2 + \tilde{q}_y^2 - \tilde{q}_y^2\tilde{q}_a^2] + \alpha(1-\tilde{q}_x\tilde{q}_a)]^2}. \quad (9b)$$

Here $\alpha = T_2/T_1 - 1 \geq 0$. (We have averaged over the resonance width Γ , which is also a random variable [13].) In case of symmetric couplings ($T_1 = T_2$), the distribution simplifies to $P(\tilde{q}_x) = \pi^{-1}(1-\tilde{q}_x^2)^{-1/2}$ [$P(\tilde{q}_x, \tilde{q}_y) = (2\pi)^{-1}(1-\tilde{q}_x^2-\tilde{q}_y^2)^{-1/2}$] with [without] TRS. In the extreme asymmetric regime $\alpha \gg 1$, the situation becomes similar to the case where only a single sticking probability is non-zero—Eq. (9) tends to a delta function distribution at $q = q_a$, cf. Eq. (8). Note however that for large but finite α , the distribution still has an appreciable width (see Fig. 2).

Dephasing. The effects of dephasing are treated phenomenologically by attaching a fictitious voltage probe to the dot [2,14]. This approach is not limited to a particular microscopic mechanism, and can describe dephasing from both intrinsic sources (i.e. from electron-electron interactions) and extrinsic sources (e.g., radiation, magnetic impurities). However, similar to a golden rule calculation [15], it does not account for possible interaction effects beyond lifetime broadening which occur at low temperatures [16]. In practice, we first replace $\varepsilon \rightarrow \varepsilon + i\hbar/2\tau_\phi$ in Eq. (6), where τ_ϕ is the phenomenological dephasing time. The imaginary part of ε models escape through the fictitious voltage probe. A correction term is then added to the conductance formula to account for the incoherent injection of electrons from the voltage probe [2,14],

$$G(\varepsilon) = |S_{12}|^2 + \frac{(1 - (SS^\dagger)_{11})(1 - (SS^\dagger)_{22})}{2 - (SS^\dagger)_{11} - (SS^\dagger)_{22}}. \quad (10)$$

The second term corresponds to incoherent transmission through the dot, and has a Breit-Wigner lineshape. As a result, the imaginary part q_y of the Fano parameter is increased. Inclusion of dephasing also changes the resonance width Γ to $\Gamma + \hbar/(2\tau_\phi)$. Writing the ratio of resonance widths without and with dephasing as

$\chi_\phi = \Gamma/(\Gamma + \hbar/(2\tau_\phi))$, we find that the change of the Fano parameters upon inclusion of dephasing is given by:

$$q_x \rightarrow \chi_\phi q_x, \quad (11a)$$

$$(q_y)^2 \rightarrow 1 - \chi_\phi + \chi_\phi(q_x^2 + q_y^2 - \chi_\phi q_x^2). \quad (11b)$$

In the presence of TRS, or in the extreme asymmetric limit, where only one sticking probability is nonzero, $q_y = 0$ in the absence of dephasing. Hence, measurement of a nonzero q_y in those cases can be used to determine τ_ϕ [17]. Calculating τ_ϕ from Eq. (11) with $q_y = 0$ in the absence of dephasing yields the relationship (2), as advertised. If TRS is broken and if both sticking probabilities are finite, q_y is already nonzero in the absence of dephasing, and a measurement of q_y cannot be used to find τ_ϕ . Note that as $\tau_\phi \rightarrow 0$, $G(\varepsilon) \rightarrow G_D$, consistent with earlier work on resonant tunneling [18].

Role of Coulomb interactions. So far we have not addressed the issue of Coulomb interactions, which are certainly present and important for small quantum dots. In this respect, we note that the time needed to traverse the quantum dot via a direct trajectory is of the same order or smaller than the inverse charging energy E_c . Hence, by the time-energy uncertainty principle, transmission via direct paths is not forbidden by Coulomb blockade. In fact, as was shown by Matveev and coworkers [19,20], Coulomb interactions actually *enhance* the probability of direct processes — both direct reflection and direct transmission [21] — at the cost of ergodic scattering. Hence, by virtue of Coulomb interactions, the dot is driven to the weak coupling regime $T_1, T_2 \ll 1$. Such an interaction-induced renormalization of the coupling between the dot and its environment may explain why in the the experiment of Ref. [5] sharp resonances were observed, despite the presence of diffraction at the point contacts. To apply our theory to this situation, it is necessary to assume that the renormalization of the scattering parameters for direct processes has already taken place. We also implicitly assumed that interactions play no further role in modifying the resonances, and that a single-particle approach is thus valid close to resonance, see Refs. [23,24].

Two interesting observations of the experiment [5] can be interpreted with the results of this letter. First, in Ref. [5], it was seen that application of a magnetic field tended to make resonances more Breit-Wigner like. Our calculation indicates that, for the generic case when both sticking probabilities are nonzero, breaking of TRS generically leads to an increase of q_y , and thus to more Breit-Wigner-like resonances, cf. Eq. (9b) (in the absence of dephasing q_y was zero without a magnetic field.) This is illustrated in the inset of Fig. 2 (compare against Fig. 6 of Ref. [5]).

Another observation in Ref. [5] was that, as a function of the gate voltage that controls the transparencies of the point contacts, the width of the observed resonances was non-monotonic. The conductance peaks started as nar-

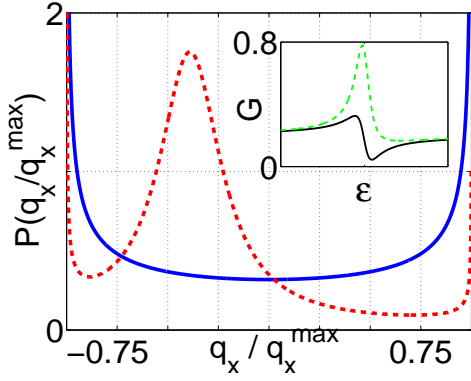


FIG. 2. Distribution of q_x in the presence of TRS for $T_2 = T_1$ (solid line) and $T_2 = 100T_1$ (dashed line). Inset: Two Fano resonances with the same q_x , but where q_y is greater for the dashed curve compared to the solid curve. (Breaking TRS causes q_y to increase on average, leading to more Breit-Wigner-like lineshapes.)

row Breit-Wigner resonances when the dot was pinched off ($G_d = 0$), then widened as the contacts were opened into resonances exhibiting the Kondo effect. As the contacts were opened further, the resonances became more narrow and had the Fano form with background conductance $G_d \simeq e^2/h$. One possible explanation is that diffraction at the contacts to the dot is strongest at intermediate point contact transparencies, leading to large sticking probabilities. (A schematic picture of the dot of Ref. [5] is shown in Fig. 1a.) To test such a scenario, we have performed numerical simulations of the system shown in Fig. 1b, using a recursive Greens function algorithm [22]. As expected, we find conductance resonances with a Fano lineshape; typical results are shown in Fig. 3a. In order to simulate how the non-monotonic resonance width in the experiment might happen, we have placed an impurity near the opening of the dot (see Fig.3), and varied its scattering strength V (V is the potential of the impurity sites in the simulation). Resonances for two values of V are shown in Figs. 3b and c; the resonance width Γ does indeed exhibit a non-monotonic dependence on V . Initially increasing V from zero has the effect of deflecting more electrons into the dot and hence increasing Γ ; larger values of V , however, cause electrons to backscatter away from the dot altogether, thus reducing Γ and suppressing the background conductance G_d .

Conclusion. Fano resonances provide a powerful tool for the study of phase coherence in transmission through quantum dots. We have shown that in certain cases, measurement of a single resonance already allows for the determination of τ_ϕ . We have also calculated the distribution of Fano parameters for a chaotic quantum dot.

We thank V. Ambegaokar, D. Goldhaber-Gordon, M. Kastner, and C. Marcus for useful discussions. A.C. acknowledges support of the Cornell Center for Materials

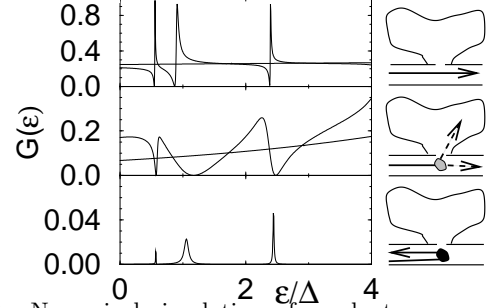


FIG. 3. Numerical simulation of conductance vs. voltage showing Fano resonances for a quantum dot with direct transmission (right). The thin line corresponds to the background conductance (i.e., when the dot is closed off). The three plots correspond to the same resonances for increasing value of the scattering strength of an impurity near the contact.

Research.

- [1] D. V. Averin and K. K. Likharev, in *Mesoscopic Phenomena in Solids*, edited by B. L. Altshuler, P. A. Lee, and R. A. Webb (North-Holland, Amsterdam, 1991).
- [2] M. Büttiker, IBM J. Res. Dev. **32**, 63 (1988).
- [3] A. Yacoby *et al.*, Phys. Rev. Lett. **74**, 4047 (1995).
- [4] E. Buks *et al.*, Phys. Rev. Lett. **77**, 4664 (1996); R. Schuster *et al.*, Nature **385**, 417 (1997).
- [5] J. Göres *et al.*, Phys. Rev. B **62**, 2188 (2000).
- [6] U. Fano, Phys. Rev. **124**, 1866 (1961); J. A. Simpson and U. Fano, Phys. Rev. Lett. **11**, 158 (1963).
- [7] E. Tekman and P. Bagwell, Phys. Rev. B **48**, 2553 (1993); J. U. Nöckel and A. D. Stone, Phys. Rev. B **50**, 17415 (1994); P. S. Deo, Solid State Commun. **107**, 69 (1998); C-M. Ryu and S. Y. Cho, Phys. Rev. B **58**, 3572 (1998).
- [8] P. A. Mello in *Mesoscopic Quantum Physics*, E. Akkermans, G. Montambaux, J.-L. Pichard, and J. Zinn-Justin, eds. (North-Holland, Amsterdam, 1995).
- [9] C. W. J. Beenakker, Rev. Mod. Phys. **69**, 731 (1997).
- [10] S. Iida, H. A. Weidenmüller and J. Zuk, Ann. Phys. **200**, 219 (1990).
- [11] C. H. Lewenkopf and H. A. Weidenmüller, Ann. Phys. **212**, 53 (1991).
- [12] M. L. Mehta, *Random Matrices* (Academic, New York, 1991).
- [13] The distribution of widths Γ after averaging over q and in the presence of TRS is given by $P = (2\Gamma_1\Gamma_2)^{-1/2}e^{-\Gamma/4\Gamma_1}e^{-\Gamma/4\Gamma_2}I_0\left(\frac{\Gamma|\Gamma_1-\Gamma_2|}{4\Gamma_1\Gamma_2}\right)$, where I_0 is a modified Bessel function, and $\Gamma_j = \frac{\Delta}{2\pi}T_j$. In the absence of TRS, one has $P = (\Gamma_1 - \Gamma_2)^{-1}(e^{\Gamma/\Gamma_1} - e^{\Gamma/\Gamma_2})$.
- [14] P. W. Brouwer and C. W. J. Beenakker, Phys. Rev. B **55**, 4695 (1997)
- [15] U. Sivan, Y. Imry and A. G. Aronov, Europhys. Lett. **28**, 115 (1994).
- [16] B. L. Altshuler *et al.*, Phys. Rev. Lett. **78**, 2803 (1997).
- [17] Using Eq. (2) and the data of ref. [5], we find dephasing times on the order of $10^{-2} - 10^{-1}$ ns, which corresponds to dephasing rates smaller than Δ . An explicit experimental study of dephasing using Fano resonances is currently planned (G. Granger, private communication).

- [18] A. D. Stone and P. A. Lee, Phys. Rev. Lett. **54**, 1196 (1985).
- [19] K. A. Matveev, Phys. Rev. B **51**, 1743 (1995).
- [20] A. Furusaki and K. A. Matveev, Phys. Rev. Lett. **75**, 709 (1995); Phys. Rev. B **52**, 16676 (1995).
- [21] P. W. Brouwer and I. L. Aleiner, Phys. Rev. Lett. **82**, 390 (1999).
- [22] H. U. Baranger *et al.*, Phys. Rev. B **44**, 10637 (1991).
- [23] G. Hackenbroich and H. A. Weidenmüller, Phys. Rev. Lett. **76**, 110 (1996).
- [24] Y. Oreg and Y. Gefen, Phys. Rev. B **55**, 13726 (1997).